INTERNATIONAL JOURNAL OF PHARMACEUTICAL SCIENCES
[ISSN: 0975-4725; CODEN(USA): IJPS00]
Journal Homepage: https://www.ijpsjournal.com

OPEN ACCESS

Research Article

Formulation and Evaluation of Glycerosomal Vesicular System for Dermal Delivery

Narendra Patel*, Kanika Dhote

Department of Pharmaceutics, Truba Institute of Pharmacy, Bhopal, Madhya Pradesh, 462038.

ARTICLE INFO

Published: 27 Nov 2026

Keywords:
Myricetin, Glycerosomes, Dermal delivery, Vesicular system, Phospholipid, Entrapment efficiency, Sustained release, Zero-order kinetics

DOI:
10.5281/zenodo.24579428

ABSTRACT

Myricetin is a bioactive flavonoid with promising antioxidant and anti-inflammatory properties; however, its poor aqueous solubility and limited dermal permeability can restrict its topical application. The present study aimed to develop a glycerosomal vesicular system to improve the dermal delivery of Myricetin. Myricetin-loaded glycerosomes (GF1–GF5) were prepared using the thin-film hydration technique by varying the phospholipid concentration while maintaining other formulation components constant. The prepared formulations were evaluated for particle size, polydispersity index (PDI), zeta potential, morphology, entrapment efficiency, and *in vitro* drug release. The optimized formulation was further subjected to release kinetic analysis. Myricetin exhibited a melting point of 358°C and a maximum absorption wavelength of 379 nm. The calibration curve demonstrated linearity in the concentration range of 10–60 µg/mL. The glycerosomal formulations showed particle sizes ranging from 193.89 to 638.9 nm and zeta potential values from −16.0 to −25.1 mV. GF1 demonstrated the smallest particle size (193.89 nm), lowest PDI (0.028), highest zeta potential (−25.1 mV), and maximum entrapment efficiency (91.64%). SEM analysis revealed spherical to near-spherical vesicles. *In vitro* release studies showed sustained Myricetin release up to 17 h, with GF1 exhibiting the highest cumulative release of 96.21%. The optimized formulation followed zero-order kinetics with an R^2 value of 0.973. The developed Myricetin-loaded glycerosomal system, particularly GF1, exhibited favorable vesicular characteristics, high drug entrapment, and sustained drug release. The findings suggest that glycerosomes may serve as a promising vesicular platform for enhancing the dermal delivery of Myricetin.

***Corresponding Author:** Narendra Patel
Address: Department of Pharmaceutics, Truba Institute of Pharmacy, Bhopal, Madhya Pradesh, 462038
Email ✉: sharmavihan7509@gmail.com

Relevant conflicts of interest/financial disclosures: The authors declare that the research was conducted in the absence of any commercial or financial relationships that could be construed as a potential conflict of interest.

INTRODUCTION

Myricetin belongs to the group of flavonoids known as flavonols. It is chemically 3, 5, 7-Trihydroxy-2-(3, 4, 5-trihydroxy phenyl)-4-chromenone. It has been suggested that myricetin is a more potent antioxidant than quercetin. In both acute and chronic models of inflammation, Wang *et al.* examined the *in vivo* anti-inflammatory effects of myricetin **(Yang *et al.*, 2019).** Myricetin had an inverse relationship with the risk of type II diabetes among different flavonoids, indicating that it may have potential anti-diabetic activity. In mice that fed a high-fat and high-sucrose diet, 0.12 % Myricetin supplementation considerably reduced hypertriglyceridemia and hypercholesterolemia, which raises the possibility that myricetin may have anti-obesity and anti-insulin resistance properties Through diverse molecular mechanisms, myricetin exhibits anticancer efficacy against different types of cancer **(Cai *et al.*, 2024).**

The vesicular systems are highly ordered assemblies of one or several concentric lipid bilayersformed when certain amphiphilic building blocks are confronted with water[5]. Biologic origin of these vesicles was first reported in 1965 by Bangham, and was given the name Bangham bodies **(Rani *et al.*, 2022).** Vesicular delivery system can be identified as highly ordered assemblies consisting of one or more concentric bilayers formed as a result of self-assembling of amphiphilic building blocks in presence of water. These systems have exceptional ability to enhance permeability of drugs. A number of novel vesicular drug delivery systems like ethosomes, liposomes, pharmacosomes, etc. have been emerged, to achieve targeted and controlled drug delivery. However, in most cases, the use of vesiclesas carriers for topical and/or transdermal administration of active principles is of little or no value due to shortcomings like instability, low entrapement efficiency and limited drug delivery efficiency **(Medhi *et al.*, 2025).**

Glycerosomes are bilayer vesicles used for dermal and transdermal drug delivery. These vesicles differ from conventional liposomes in bilayer fluidity, formed by the addition of phospholipids and varying concentrations of glycerol (10-30 % v/v) **(Gupta et al., 2020).** These are so named, as they contain high amount of glycerol. These vesicles deliver the active ingredients to skin with high efficiency **(Ashtianiet al.,2016).** Glycerosomes are found to be more stable and possess greater fluidity then liposomes and hence are predominantly used as topical drug delivery systems. Glycerol ameliorates the deformability index of liposomal bilayers, thus enhancing skin penetration **(Zhang et al., 2017).**

For myricetin, incorporation into a glycerosomal vesicular system may overcome some of the limitations associated with its conventional dermal administration. Encapsulation of myricetin within glycerosomes may improve its apparent solubility and facilitate its transport into the skin while protecting the active constituent from premature degradation **(Pozos-Nonato *et al.*, 2023).** Furthermore, the flexible nature of glycerosomal vesicles may promote closer interaction with the skin surface and enhance drug deposition in the desired skin layers. Such an approach may be particularly beneficial for exploiting the antioxidant and anti-inflammatory properties of myricetin in localized dermal applications **(Abdallah *et al.*, 2025).**

Therefore, the present study was undertaken to formulate and evaluate a myricetin-loaded glycerosomal vesicular system for enhanced dermal delivery. The study aims to develop a suitable glycerosomal carrier capable of improving the physicochemical and biopharmaceutical characteristics of myricetin and enhancing its dermal delivery.

MATERIAL AND METHODS

2.1 Chemicals

Myricetin, were obtained from ZES Bioscience. Merck Life Science Pvt. Ltd., Bengaluru, India provided the Glycerol, Ethanol and Methanol. HiMedia Laboratories Pvt. Ltd., Mumbai, India provided the Soya Lecithin, Potassium Dihydrogen Phosphate and Disodium Hydrogen Phosphate while Loba Chemie Pvt. Ltd., Mumbai, India supplied Tween 80.

2.2 Pre-formulation studies

Pre-formulation studies for Myricetin are a vital step in developing an effective topical formulation. These studies assess key properties such as solubility, stability, and compatibility with excipients. Understanding

these characteristics helps in selecting suitable formulation components and optimizing the drug's bioavailability, efficacy, and shelf life. The goal is to generate essential data to support the development of a stable and effective myricetin-based product **(Robinson *et al.,* 2015).**

2.2.1 Organoleptic Properties

Myricetin was evaluated for its physical appearance including color, odor, and nature. **(Wang *et al.,* 2024).**

2.2.2 Solubility study

The solubility of Myricetin was determined in different solvents such as distilled water, methanol, ethanol, chloroform, and DMSO. Excess quantity of drug was added to each solvent and shaken for 24 hours at room temperature. The solutions were filtered and visually examined for solubility characteristics. Each mixture was thoroughly stirred to promote dissolution, and then visually examined to assess the extent of solubility. Particular attention was given to the presence of any undissolved particles, as well as changes in the clarity, color, or consistency of the solution. This method provided a straightforward yet informative assessment of Myricetin solubility profile, aiding in the identification of the most suitable solvent for further formulation development **(Cheney *et al.,* 2010).**

2.2.3 pH determination

The pH of the Myricetin solution was measured to evaluate its acid-base properties, which play a crucial role in determining the drug's solubility, stability, and compatibility with other formulation components. Prior to measurement, the pH meter was calibrated using standard buffer solutions to ensure accuracy **(Jin *et al.,* 2028).**

2.2.4 Melting Point

A small quantity of Myricetin was gently packed into a thin capillary tube for the purpose of determining its melting point by using melting point apparatus, and the temperature was gradually increased at a controlled rate **(Yalkowsky and Alantary 2018).**

2.2.5 Spectroscopic Analysis and Calibration of Myricetin

• Lambda (λ) max analysis

A stock solution of Myricetin was prepared by dissolving the drug in methanol to achieve a concentration of 1 mg/mL. From this stock, a working standard solution of 100 µg/mL was obtained through appropriate dilution using the same solvent. Further dilution was carried out to prepare a working standard solution of suitable concentration. The diluted solution was then analyzed using a Shimadzu 1700 double beam UV-Visible spectrophotometer, scanned in the wavelength range of 200–400 nm using a UV–Visible spectrophotometer against methanol as blank. The wavelength at which maximum absorbance was observed was recorded as the λmax of Myricetin **(Azeem *et al.,* 2023).**

• Standard calibration curve analysis

A standard calibration curve of Myricetin was prepared using methanol as solvent. From the prepared stock solution, appropriate aliquots were withdrawn and diluted to obtain concentrations within the Beer–Lambert's law range. The absorbance of each concentration was measured at the determined λmax using a UV–Visible spectrophotometer. A graph was plotted between concentration (µg/mL) and absorbance values to obtain the calibration curve. The linearity of the method was evaluated by calculating the regression equation and correlation coefficient (R^2), which indicated the relationship between concentration and absorbance **(William*et al.,* 2026).**

2.2.6 Preparation of calibration curve

A standard stock solution of Myricetin was prepared by accurately weighing 10 mg of Myricetin and dissolving it in methanol in a 10 mL volumetric flask to obtain a concentration of 100µg/mL. From this stock solution, a secondary stock solution of 100µg/mL was prepared by transferring 1 mL into a 10 mL volumetric flask and making up the volume with methanol. Aliquots of the secondary stock solution were further diluted with methanol to obtain concentrations of 10, 20, 30, 40, 50 and 60µg/mL. The absorbance of each prepared solution was measured at the predetermined λmax of

Myricetin using a UV–Visible spectrophotometer against methanol as blank. A calibration curve was plotted by taking concentration on the X-axis and absorbance on the Y-axis. The linear regression equation and correlation coefficient (R^2) were calculated to evaluate the linearity of the method according to Beer–Lambert's law **(Azadeh *et al.*, 2017).**

2.2.7 Fourier Transform Infrared (FT-IR) Spectroscopy of Myricetin

FT-IR spectroscopy was used to identify the distinctive functional groups in myricetin and establish its chemical structure. The FT-IR spectra were acquired on an FT-IR spectrophotometer using the potassium bromide (KBr) pellet method. Approximately 1-2 mg of myricetin was completely mixed with 100-200 mg of dry spectroscopic-grade KBr, finely powdered, and compressed into a transparent pellet using hydraulic pressure. The spectrum was collected at room temperature in the wavenumber region of 4000-400 cm^{-1}. The acquired absorption bands were examined and attributed to the respective functional groups, including hydroxyl (-OH), carbonyl (C=O), aromatic C=C, and C-O stretching vibrations, to establish myricetin's identity and purity **(Davis *et al.*, 2010).**

2.3 Preparation of Glycerosomes

Myricetin-loaded glycerosomes (GS1–GS5) were prepared by the thin-film hydration technique. Myricetin (30 mg), cholesterol (40 mg), and phospholipid (10–50 mg) were dissolved in methanol (10 mL) and chloroform (10 mL) and evaporated under reduced pressure at 40°C to form a thin lipid film. The film was vacuum-dried overnight and hydrated with 15 mL of PBS (pH 6.8) containing 10% v/v glycerol at 40°C for 1 h with continuous stirring. The resulting vesicles were probe-sonicated to reduce particle size and centrifuged at 1500 rpm for 10 min at 4°C to remove unencapsulated drug. The purified glycerosomal dispersions were lyophilized and stored at 4°C until further evaluation. GS1–GS5 differed only in phospholipid concentration (10–50 mg), while other formulation components were kept constant **(Rani *et al.*, 2016).**

Table 1: Composition of Glycerosomes Formulation

Formulation code	Myricetin Drug (mg)	Phospholipid (mg)	Glycerol (%)	Cholesterol (mg)	Methanol (ml)	Chloroform (ml)	PBS 6.8 (ml)
GS 1	30.0	10.0	10.0	40.0	10.0	10.0	15.0
GS 2	30.0	20.0	10.0	40.0	10.0	10.0	15.0
GS 3	30.0	30.0	10.0	40.0	10.0	10.0	15.0
GS 4	30.0	40.0	10.0	40.0	10.0	10.0	15.0
GS 5	30.0	50.0	10.0	40.0	10.0	10.0	15.0

2.4 Characterization of Vesicular System

2.4.1 Physical appearance

The physical appearance of the Myricetin -loaded glycerosomes was thoroughly evaluated to determine their quality and stability. Visual inspection was carried out to assess parameters such as shape, uniformity, and color of the vesicles **(Schaefer and Thompson 2014).**

2.4.2 Particle Size

The average vesicle size and polydispersity index of the prepared glycerosomes were determined using dynamic light scattering (DLS) technique **(Blott and Pye 2012).**

2.4.3 Zeta Potential

The zeta potential of myricetin -loaded glycerosomes was measured using a Malvern Zetasizer (Malvern Instruments) **(Bhattacharjee, 2016).**

2.4.4 Scanning Electron Microscopy (SEM) Analysis

The surface morphology and structural features of myricetin-loaded glycerosomes were investigated using Scanning Electron Microscopy (SEM) **(Mohammed and Abdullah 2018).**

2.4.5 Drug Entrapment Efficiency

To accurately determine the entrapment efficiency of myricetin in glycerosomes, 10 mL of the myricetin-

loaded glycerosomal dispersion was combined with 5 mL of methanol in a volumetric flask. The mixture was vortexed for one minute to ensure complete disruption of the vesicles and release of the encapsulated drug. The solution was then diluted to a final volume of 10 mL with an appropriate solvent. After filtration, the concentration of myricetin was measured using UV-Visible spectrophotometry. These results were used to calculate the entrapment efficiency, providing an assessment of the drug loading capacity within the glycerosomal formulation **(Dhakar *et al.*, 2010).**

The entrapment efficiency is then determined using the formula:

Entrapment efficiency % = Total drug conc. - Supernatant drug conc. / total drug conc. × 100

This method provides an accurate estimation of how much myricetin was successfully encapsulated within the glycerosomes.

2.5 *In Vitro* Drug Release Study

In vitro drug release studies were carried out using a Franz diffusion cell fitted with a dialysis membrane. The receptor compartment was filled with phosphate buffer (pH 7.4) and maintained at 37 ± 0.5°C under continuous magnetic stirring (500 rpm) to simulate physiological conditions. An accurately weighed quantity of the Myricetin-loaded glycerosomal formulation was placed in the donor compartment. At predetermined time intervals (0.2, 4, 6, 8, 10, 12, 14, and 17 h), aliquots were withdrawn from the receptor compartment and immediately replaced with an equal volume of fresh phosphate buffer to maintain sink conditions. The collected samples were analyzed using a UV–Visible spectrophotometer at the predetermined λmax of Myricetin, and the cumulative percentage drug release was calculated. The release profile of the optimized Myricetin-loaded glycerosomal formulation was compared with that of the plain Myricetin suspension to evaluate the enhancement in drug release and dermal delivery potential provided by the glycerosomal vesicular system **(Briuglia *et al.*, 2010).**

Drug Release Kinetic Studies

To elucidate the mechanism of drug release from the Myricetin-loaded glycerosomal formulation, the *in vitro* release data were fitted to various mathematical kinetic models, including Zero-order, First-order, Higuchi, and Korsmeyer–Peppas models.

The kinetic models were expressed as follows:

1. Zero-order model

$$Q_t = Q_0 + K_0 t$$

2. First-order model

$$\log\ Q_t = \log\ Q_0 - \frac{K_1 t}{2.303}$$

3. Higuchi model

$$Q = K_H \sqrt{t}$$

4. Korsmeyer–Peppas model

$$\frac{M_t}{M_\infty} = K_{KP} t^n$$

The regression coefficient (R^2) values obtained from each kinetic model were compared, and the model showing the highest R^2 value was considered to best describe the drug release kinetics. The release exponent (n) obtained from the Korsmeyer–Peppas model was used to determine the mechanism of drug release, where $n \leq 0.45$ indicates Fickian diffusion, $0.45 < n < 0.89$ indicates anomalous (non-Fickian) transport, $n = 0.89$ indicates Case II transport, and $n > 0.89$ indicates Super Case II transport. This kinetic evaluation provided insight into the release behavior and mechanism of Myricetin from the glycerosomal vesicular system

RESULTS AND DISCUSSION

3.1 Pre-formulation study of drug

3.1.1 Organoleptic properties

Table 2: Organoleptic Properties of Myricetin

Drug	Organoleptic properties	Observation
Myricetin	Color	Yellow to yellowish-brown
	Odor	Odorless
	Appearance	Crystalline powder
	State	Solid

3.1.2 Melting point

Table 3: Melting Point and pH of Myricetin

Drugs	Observed (Melting point)	Reference (Melting point)	Observed (pH)	Reference (pH)
Myricetin	358°C	357–360°C	6.4	6.0 – 7.0

3.1.3 Calibration curve of Myricetin

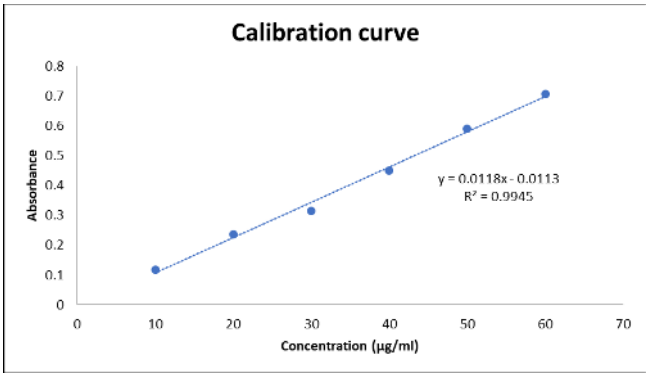

Graph 1: Calibration Curve of Myricetin

3.1.2 Functional group identified by Infra-Red spectroscopy

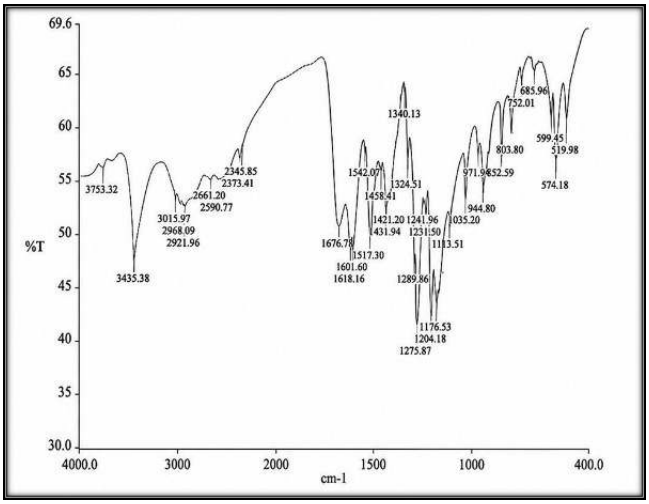

Graph 2: FTIR Study of Myricetin

Table 4: Interpretation of IR Spectrum of Myricetin

Peak Obtained (cm^{-1})	Reference Range (cm^{-1})	Functional Group (Vibration)	Name of Functional Group
3448.15	3500- 3400	N-H stretching	Primary Amine
3015.97	3100-3000	C-H stretching	Alkene
2968.09	3000-2840	C-H stretching	Alkane
2590.77	2600-2550	S-H stretching	Thiol
1676.78	1690-1640	C=N stretching	Imine / Oxime

3.2 Characterization of drug loaded Glycerosome formulation

3.2.1 Physical Appearance

Table 5: Physical Appearance Glycerosome Formulation

Parameter	Observation
Color	Colorless to pale yellow
Odor	Characteristic
Appearance	Homogeneous
State	Liquid dispersion

3.2.2 Particle size (PS) of glycerosome formulation (GS)

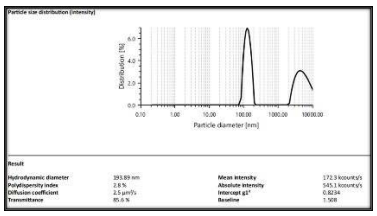

Graph 3: PS of GS F1

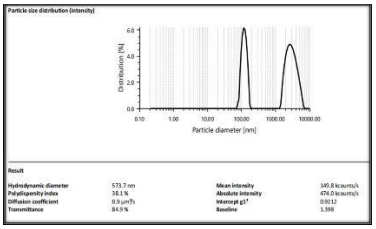

Graph 4: PS of GS F2

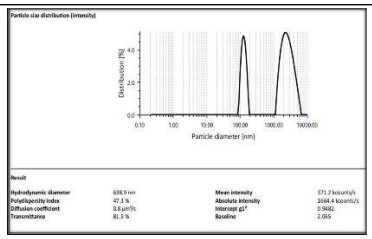

Graph 5: PS of GS F3

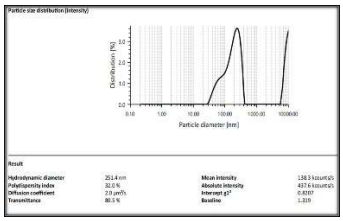

Graph 6: PS of GS F4

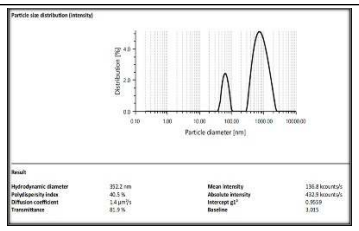

Graph 7: PS of GS F5

3.2.3 Zeta potential (ZP) of Glycerosome (GS)

Table 6: Particle Size (PS) and Zeta Potential (ZP) of Glycerosome (GS)

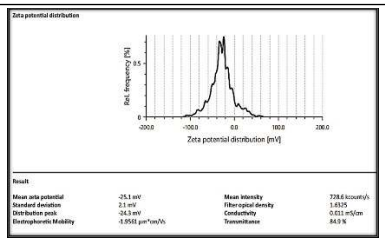

Graph 8: ZP of GS F1

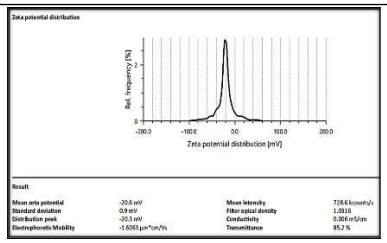

Graph 9: ZP of GS F2

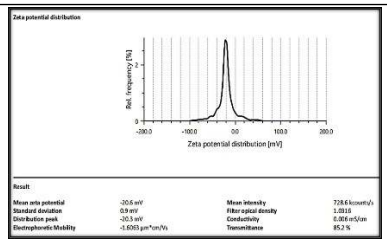

Graph 10: ZP of GS F3

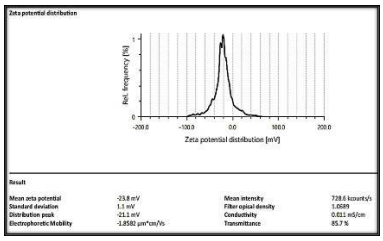

Graph 11: ZP of GS F4

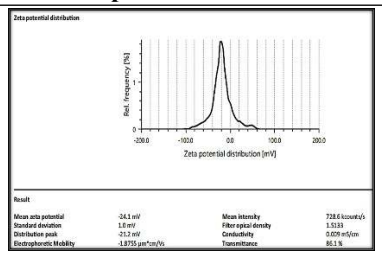

Graph 12: ZP of GS F5

Formulation code	Particle size (nm)	PI Value %	Zeta potential (mV)
PS of GS F1	**193.89 nm**	**2.8 %**	**-25.1mV**
PS of GS F2	573.7 nm	38.1 %	-16.0 mV
PS of GS F3	638.9 nm	47.3 %	-20.6 mV
PS of GS F4	251.4 nm	32.0 %	-23.8 mV
PS of GS F5	352.2 nm	40.5 %	-24.1 mV

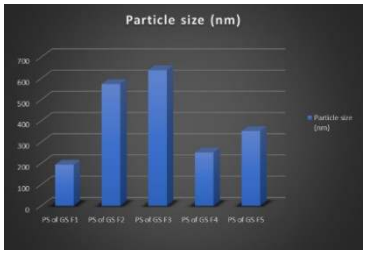

Graph 13: Graphical Data of Particle size of Glycerosome



Graph 14: Graphical Data of Zeta potential of Glycerosome

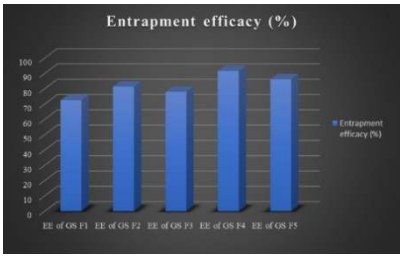

Graph 15: Graphical Data of EE of Glycerosome

3.2.4 SEM analysis of Optimized formulation

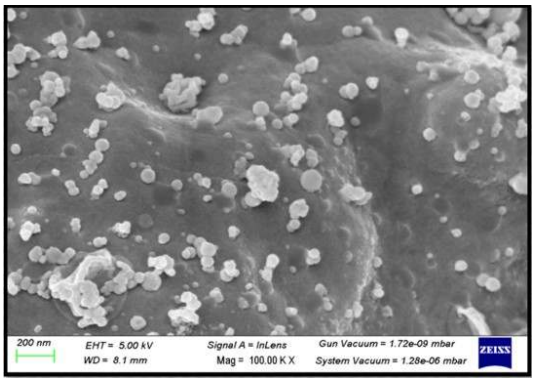

Figure 1: SEM Analysis

3.3 *In vitro* drug release study of all formulations

Table 8: *In vitro* Drug Release Study of All Formulations

Time (hrs)	Cumulative % drug release study				
	GS 1	GS 2	GS 3	GS 4	GS 5
0	0	0	0	0	0
2	18.42	16.06	15.38	14.75	17.20
4	31.65	28.42	26.89	25.73	30.18
6	45.72	40.36	38.25	37.12	43.56
8	58.64	51.84	49.72	47.93	56.30
10	70.83	63.25	61.46	59.72	67.15
12	80.96	73.18	71.35	69.42	77.64
14	88.74	82.06	80.12	78.36	85.90
17	96.21	89.19	87.45	85.72	92.68

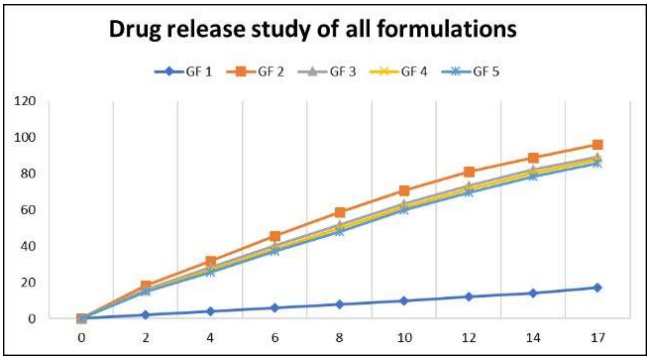

Graph 16: Drug Release Study of All Formulations

Table 9: Release Kinetics Study of Optimized Glycerosomes Formulation

Time (Hr)	cumulative % drug released	% drug remaining	Square root time	log Cumu % drug remaining	log time	log Cumu % drug released
0	0	100	0.000	2.000	0.000	0.000
2	18.42	81.58	1.414	1.912	0.301	1.265
4	31.65	68.35	2.000	1.835	0.602	1.500
6	45.72	54.28	2.449	1.735	0.778	1.660
8	58.64	41.36	2.828	1.617	0.903	1.768
10	70.83	29.17	3.162	1.465	1.000	1.850
12	80.96	19.04	3.464	1.280	1.079	1.908
14	88.74	11.26	3.742	1.052	1.146	1.948
17	96.21	3.79	4.123	0.579	1.230	1.983

Table 10: Correlation Value (R^2 Value)

Formulation	Model	Kinetic parameter values
GSF1	Zero Order	$R^2 = 0.973$
	First Order	$R^2 = 0.912$
	Higuchi	$R^2 = 0.877$
	Korsmeyerpeppas	$R^2 = 0.849$

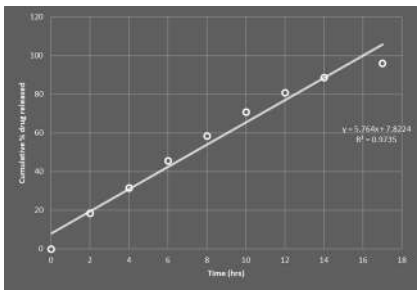

Graph 17: Zero order kinetic model

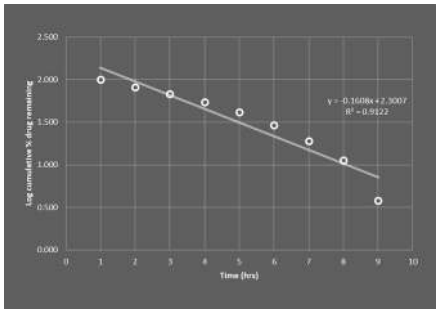

Graph 18: First Order kinetic model

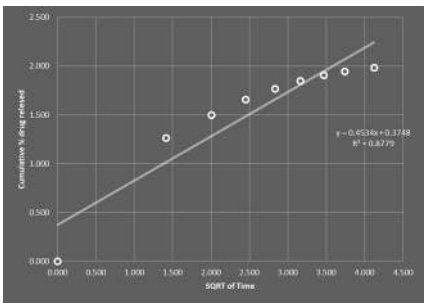

Graph 19: Higuchi model

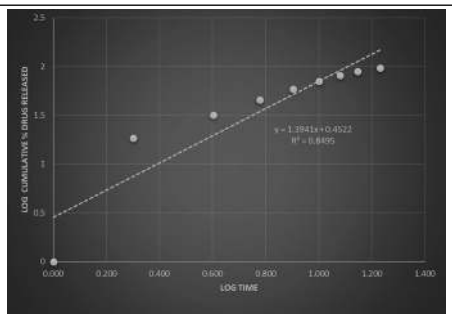

Figure 20: Korsmeyer peppas

DISCUSSION

The present study successfully demonstrated the development of a Myricetin-loaded glycerosomal vesicular system for dermal delivery. Myricetin exhibited suitable organoleptic properties, a melting point of 358°C, and a λmax of 379 nm, confirming its identity and suitability for further formulation studies. The calibration curve showed good linearity over the concentration range of 10–60 µg/mL, supporting the applicability of the UV spectrophotometric method for drug estimation. Glycerosomal formulations exhibited particle sizes of 193.89–638.9 nm and zeta potentials ranging from −16.0 to −25.1 mV. Among the formulations, GF1 showed the smallest particle size (193.89 nm), lowest PDI (0.028), highest zeta potential (−25.1 mV), and maximum entrapment efficiency (91.64%),

indicating favorable vesicular characteristics. SEM confirmed the formation of spherical to near-spherical nanosized vesicles. The formulations demonstrated sustained Myricetin release over 17 h, with GF1 showing the highest cumulative drug release of 96.21%. Release kinetics indicated that GF1 followed a zero-order release model ($R^2 = 0.973$). Overall, GF1 demonstrated the most favorable formulation characteristics and sustained release behavior, indicating the potential of glycerosomes as a promising carrier for dermal delivery of Myricetin.

CONCLUSION

The present study successfully developed and evaluated Myricetin-loaded glycerosomes as a potential dermal drug delivery system. Preformulation studies confirmed the identity and suitability of Myricetin, with good analytical linearity over 10–60 µg/mL. The prepared glycerosomal formulations showed nanosized vesicles, acceptable surface charge, and effective drug entrapment. Among all formulations, GSF1 was optimized, exhibiting the smallest particle size (193.89 nm), low PDI, highest zeta potential (−25.1 mV), and maximum entrapment efficiency (91.64%). SEM confirmed spherical to near-spherical vesicular morphology. GSF1 provided 96.21% drug release over 17 h and followed zero-order kinetics ($R^2 = 0.973$), indicating sustained and controlled drug release. Overall, the findings suggest that Myricetin-loaded glycerosomes may serve as a promising approach for enhancing dermal delivery and warrant further investigation through skin permeation, stability, and in vivo studies.

REFERENCES

1. Yang ZJ, Wang HR, Wang YI, Zhai ZH, Wang LW, Li L, Zhang C, Tang L. Myricetin attenuated diabetes-associated kidney injuries and dysfunction via regulating nuclear factor (erythroid derived 2)-like 2 and nuclear factor-κB signaling. Frontiers in Pharmacology. 2019 Jun 11;10:647.
2. Cai T, Song X, Xu X, Dong L, Liang S, Xin M, Huang Y, Zhu L, Li T, Wang X, Fang Y. Effects of plant natural products on metabolic-associated fatty liver disease and the underlying mechanisms: A narrative review with a focus on the modulation of the gut microbiota. Frontiers in cellular and infection microbiology. 2024 Feb 20;14:1323261.
3. Rani D, Sharma V, Singh P, Singh R. Glycerosomes: A novel vesicular drug delivery system. Research Journal of Pharmacy and Technology. 2022 Feb 1;15 (2):921-6.
4. Medhi J, Thalluri C, Vasam M, Bukke SP. The future of vesicular drug delivery: transferosomes in therapeutic advancement—applications, innovations and challenges. BioMedical Engineering OnLine. 2025 Dec 2;25 (1):1.
5. Gupta P, Mazumder R, Padhi S. Glycerosomes: advanced liposomal drug delivery system. Indian J. Pharm. Sci. 2020 May 1;82 (3):385-97.
6. Ashtiani HA, Bishe P, Lashgari NA, Nilforoushzadeh MA, Zare S. Liposomes in cosmetics. J. Skin Stem Cell. 2016 Jun;3 (3):e65815.
7. Zhang K, Zhang Y, Li Z, Li N, Feng N. Essential oil-mediated glycerosomes increase transdermal paeoniflorin delivery: Optimization, characterization, and evaluation in vitro and in vivo. International journal of nanomedicine. 2017 May 5:3521-32.
8. Pozos-Nonato S, Domínguez-Delgado CL, Campos-Santander KA, Benavides AA, Pacheco-Ortin SM, Higuera-Piedrahita RI, Resendiz-González G, Molina-Trinidad EM. Novel nanotechnological strategies for skin anti-aging. Current pharmaceutical biotechnology. 2023 Sep 1;24 (11):1397-419.
9. Abdallah, M. H., Shahien, M. M., El-Horany, H. E. S., & Ahmed, E. H. (2025). Modified phospholipid vesicular gel for transdermal drug delivery: the influence of glycerin and/or ethanol on their lipid bilayer fluidity and penetration characteristics. *Gels*, *11*(5), 358.
10. Robinson K, Mock C, Liang D. Pre-formulation studies of resveratrol. Drug development and industrial pharmacy. 2015 Sep 2;41 (9):1464-9.
11. Wang J, Wang XS, Zhang Z, Zhou DY, Huang XH, Qin L. Comprehensive insights into the organoleptic characteristics attributes of "HuangYuXiang": Integration of volatilomics, sensomics, macrogenomics, lipidomics, and

metabolomics. Food Chemistry. 2024 Dec 1;460:140409.

12. Cheney ML, Shan N, Healey ER, Hanna M, Wojtas L, Zaworotko MJ, Sava V, Song S, Sanchez-Ramos JR. Effects of crystal form on solubility and pharmacokinetics: a crystal engineering case study of lamotrigine. Crystal Growth & Design. 2010 Jan 6;10 (1):394-405.
13. Jin H, Qin Y, Pan S, Alam AU, Dong S, Ghosh R, Deen MJ. Open-source low-cost wireless potentiometric instrument for pH determination experiments.
14. Yalkowsky SH, Alantary D. Estimation of melting points of organics. Journal of pharmaceutical sciences. 2018 May 1;107 (5):1211-27.
15. Azeem N, Beatrice C, Vassallo A, Pesce F, Davide G, Guido C, Rossi PhD R. Comparative analysis of different methodologies to calculate lambda (λ) based on extensive and systemic experimentation on a hydrogen internal combustion engine. In-WCX SAE World Congress Experience 288442 2023 Apr 11.
16. Williams PJ, Thushara N, Yousefi A, Mundschutz H, Hore DK, McIndoe JS. Faster, simpler, and more precise calibration curves: Expanding the scope of continuous calibration. Analytica Chimica Acta. 2026 Feb 20:345285.
17. Azadeh M, Gorovits B, Kamerud J, MacMannis S, Safavi A, Sailstad J, Sondag P. Calibration curves in quantitative ligand binding assays: recommendations and best practices for preparation, design, and editing of calibration curves. The AAPS journal. 2017 Dec 27;20 (1):22.
18. Davis R, Mauer LJ. Fourier transform infrared (FT-IR) spectroscopy: a rapid tool for detection and analysis of foodborne pathogenic bacteria. Current research, technology and education topics in applied microbiology and microbial biotechnology. 2010 Jan 1;2:1582-94.
19. Rani D, Singh C, Kumar A, Sharma VK. Formulation development and in-vitro evaluation of minoxidil bearing glycerosomes. Am J Biomed Res. 2016;4:27-37.
20. Schaefer LM, Thompson JK. The development and validation of the physical appearance comparison scale-revised (PACS-R). Eating behaviors. 2014 Apr 1;15 (2):209-17.
21. Blott SJ, Pye K. Particle size scales and classification of sediment types based on particle size distributions: Review and recommended procedures. Sedimentology. 2012 Dec;59 (7):2071-96.
22. Bhattacharjee S. DLS and zeta potential–what they are and what they are not?. Journal of controlled release. 2016 Aug 10;235:337-51.
23. Mohammed A, Abdullah A. Scanning electron microscopy (SEM): A review. InProceedings of the 2018 international conference on hydraulics and pneumatics—HERVEX, Băile Govora, Romania 2018 Nov 7 (Vol. 2018, pp. 7-9).
24. Dhakar RC, Maurya SD, Sagar BP, Bhagat S, Prajapati SK, Jain CP. Variables influencing the drug entrapment efficiency of microspheres: A pharmaceutical review. Der Pharmacia Lettre. 2010;2 (5):102-16.
25. Briuglia ML, Rotella C, McFarlane A, Lamprou DA. Influence of cholesterol on liposome stability and on *in vitro* drug release. Drug delivery and translational research. 2015 Jun;5 (3):231-42.

HOW TO CITE: Narendra Patel, Kanika Dhote, Formulation and Evaluation of Glycerosomal Vesicular System for Dermal Delivery, Int. J. of Pharm. Sci., 2026, Vol 4, Issue 11, 5341-5351. https://doi.org/10.5281/zenodo.24579428